

# ACQUISITION AND PROCESSING REPORT

SKYTEM HELICOPTER EM SURVEY

HAYES CREEK, NT

Report for

**Rockland Resources**



# **ACQUISITION AND PROCESSING REPORT: SKYTEM HELICOPTER EM SURVEY OVER HAYES CREEK, NT.**

## **1. SURVEY SPECIFICATIONS**

### **1.1 General**

Table 1 below lists the basic survey information.

**Table 1 General survey information**

SkyTEM Job Number	AUS_10027
Survey Company	SkyTEM Australia Pty Ltd
Reporting Period	August 2017
Client	Rockland Resources
Terrain Clearance	45 - 60 m (nominal)
Line Kilometres	13.7 km
Line Direction	Variable
Line Spacing	Variable
Datasets Acquired	Time-domain EM Magnetics
EM System	SkyTEM (Interleaved Low Moment and High Moment)
Helicopter Company	Frontier Helicopters Pty Ltd
Helicopter Type	AS350 B2
Helicopter Registration	VH-FBQ
Navigation	Real Time DGPS. Base GPS data was recorded as a backup.
Coordinate System	MGA52 / GDA94

## 1.2 Flight Path

The survey flight lines for the survey blocks are shown in Figure 1.

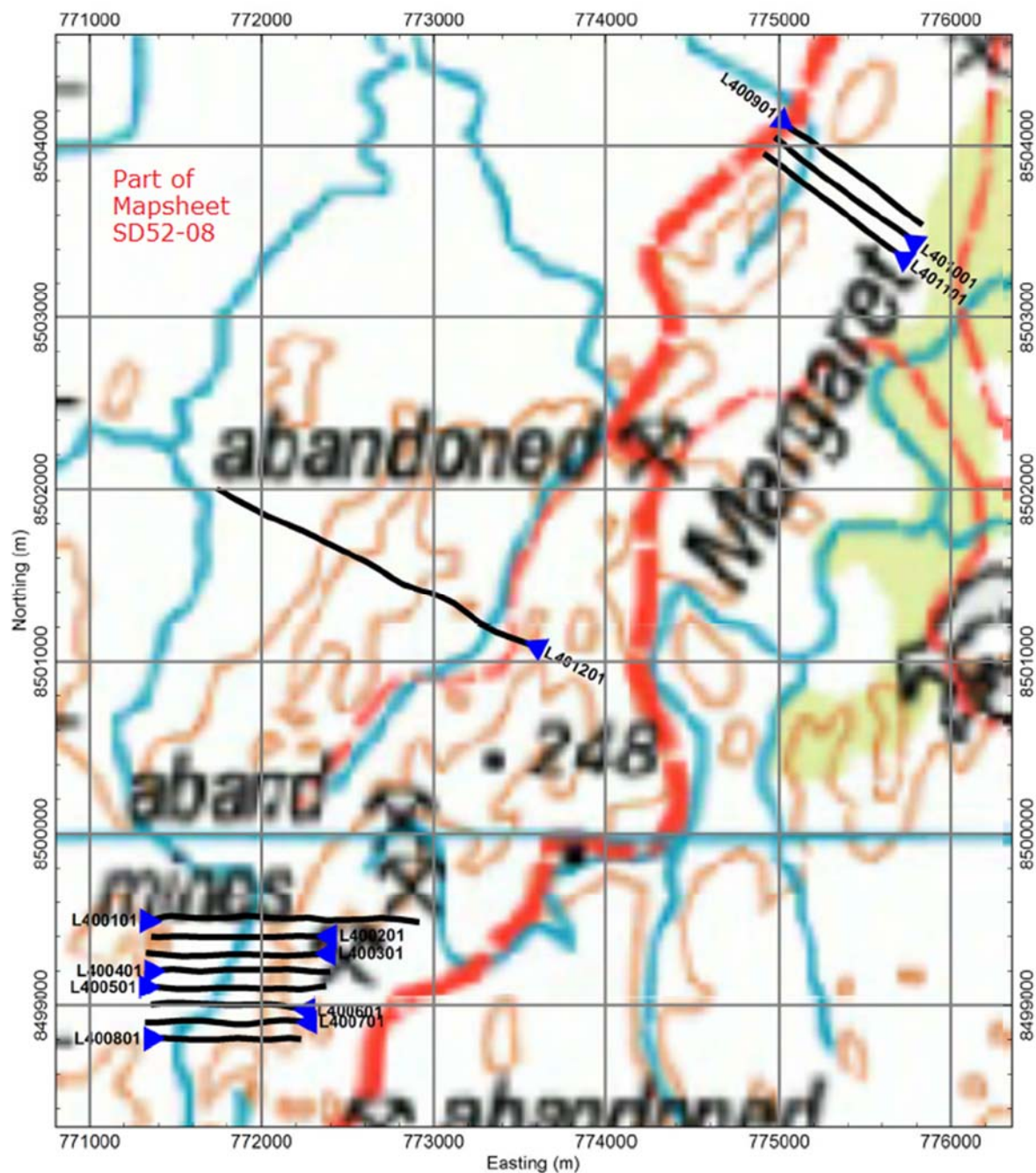


**Figure 1 SkyTEM flight path map.**

## 1.3 Logistics

The survey was flown from an operating base at Hayes Creek, NT. The survey was conducted on the 26<sup>th</sup> August 2017.

No environmental or safety issues were reported.

Date: 13 January 2018	Doc. No: AUS_10027	Page 3 of 31
-----------------------	-----------------------	--------------

## 1.4 Personnel

A list of the personnel for the survey is provided in Table 2.

**Table 2 Survey personnel**

Field	
Crew Chief	Brett Rees
Field Tech	Wade Markow
Pilot	Morgan Inglis
Office	
Data Processing	SkyTEM Australia
Reporting	SkyTEM Australia (Brendan Coleman) <a href="mailto:bc@skytem.com">bc@skytem.com</a>

## 2. ACQUISITION SYSTEM INSTRUMENTS AND PARAMETERS

### 2.1 Physical Configuration

The geometry of the system used during acquisition is represented in Figure 2:

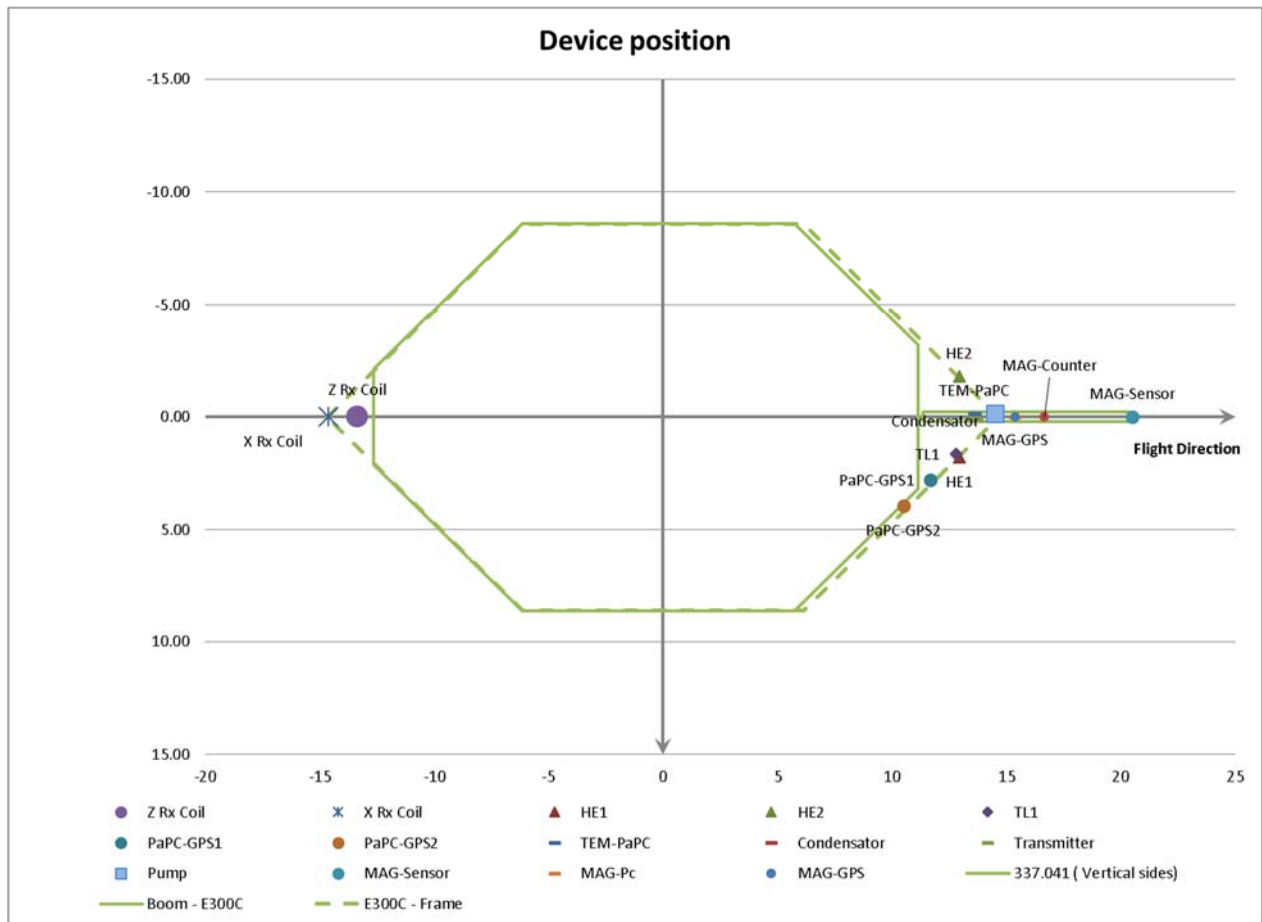


**Figure 2 Schematic of the SkyTEM312 System**

The XYZ coordinates of the instruments relative to the centre of the transmitter loop are provided in Table 3.

**Table 3 Relative positions of system instruments. The Z-axis is positive below the Tx loop wire. Positive X and Y-axes are in the flight direction and to the starboard side respectively, forming a right-handed coordinate system.**

ITEM	DESCRIPTION	SkyTEM <sup>312</sup>		
		X(m)	Y(m)	Z(m)
Z-coil	EM Z-axis sensor	-13.36	0.00	-2.00
X-coil	EM X-axis sensor	-14.65	0.00	-0.04
TL1/TL2	Tiltmeter 1 & 2 (measures tilts from horizontal with respect to both X and Y axes)	12.79	1.64	-0.12
HE1	Laser Altimeter 1	12.94	1.79	-0.12
HE2	Laser Altimeter 2	12.94	-1.79	-0.12
PaPC-GPS1	GPS 1 Antenna (Standard)	11.68	2.79	-0.16
PaPC-GPS2	GPS 2 Antenna (RTK DGPS)	10.51	3.95	-0.16

## 2.2 Transmitter Parameters

A summary of the transmitter specifications is provided in Table 4, with details of the transmitter waveforms for the different moment configurations given in Table 6 and Table 7, and shown in Figure 3 and Figure 4.

**Table 4 Summary of transmitter specifications**

TRANSMITTER SPECIFICATIONS	
Tx ID = 30	SkyTEM <sup>312</sup>
Transmitter (Tx) Loop Area	337.0 m <sup>2</sup>
Transmitter Moments	LM + HM
Number of Transmitter Loop Turns	2 turn (LM) 12 turns (HM)
Nominal Peak Current	6.0 A (LM) 119 A (HM)
Peak Moment	~4,090 Am <sup>2</sup> (LM) ~487,000 Am <sup>2</sup> (HM)
Nominal Tx/Rx Frame Height	~45 m

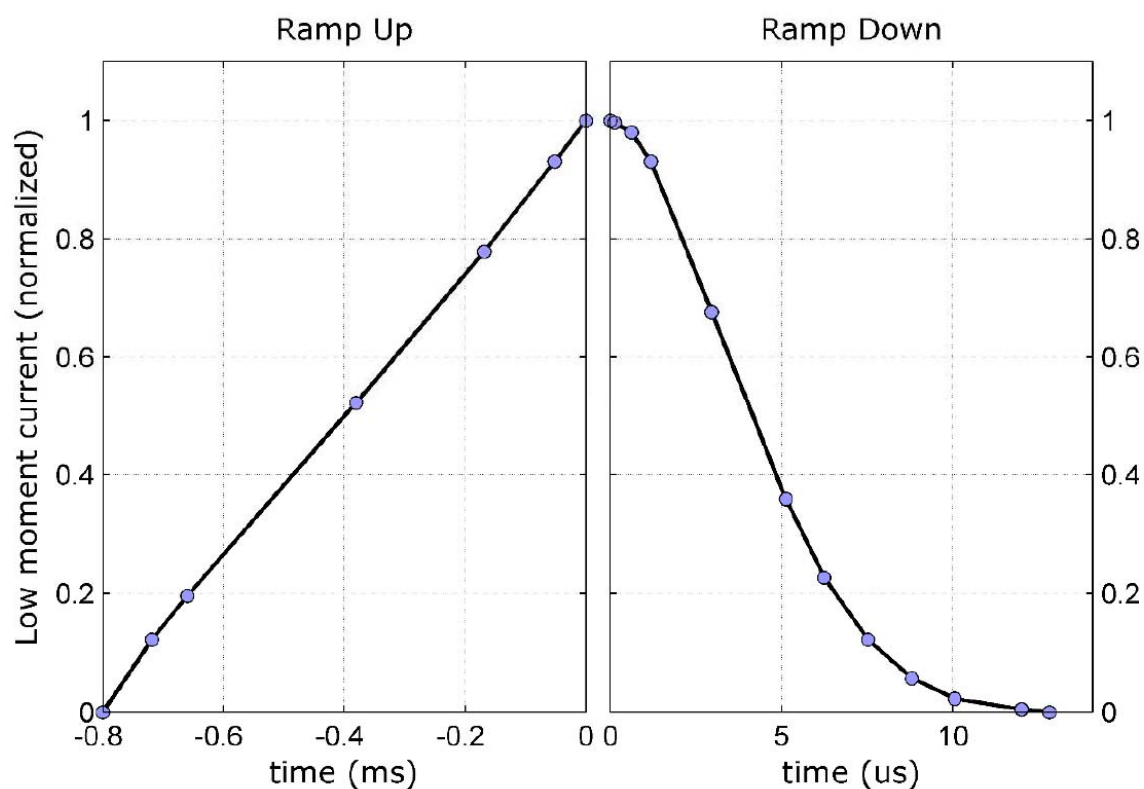
**Table 5 Transmitter waveform specifications**

TRANSMITTER WAVEFORM	
Base Frequency	275 Hz (LM) 25 Hz (HM)
Tx Duty Cycle	44% (LM), 25% (HM)
Tx Waveforms	Linear rise, linear ramp-off, Bipolar (LM)
	Pseudo-rectangular, linear ramp-off. Bipolar (HM)
Tx ON-Time	0.8 ms and 5.0 ms
Tx OFF-Time	1.018 ms and 15.0 ms

**Table 6 Detailed SkyTEM<sup>312</sup> LM transmitter current waveform**

Time[s]	Amplitude
-8.0000E-04	0.0000E+00
-7.1847E-04	1.2266E-01
-6.5990E-04	1.9609E-01
-3.8062E-04	5.2228E-01
-1.6838E-04	7.7866E-01

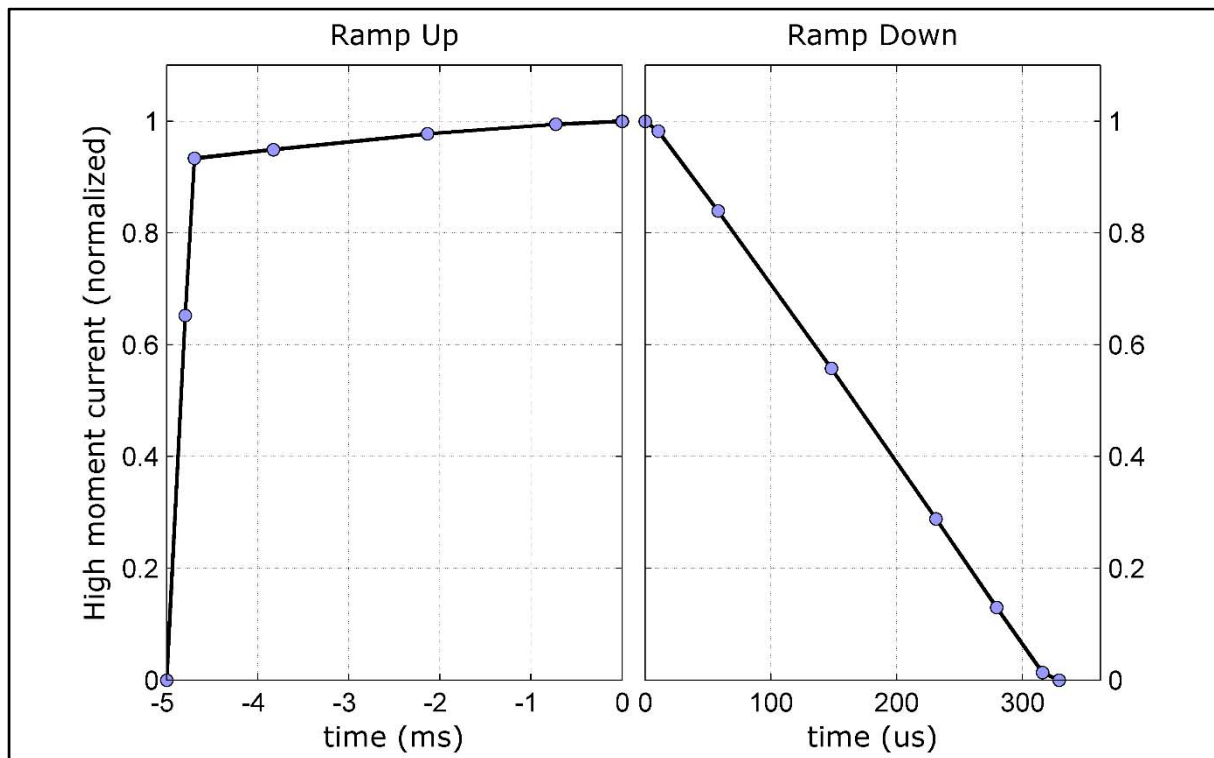
-5.1442E-05	9.3110E-01
0.0000E+00	1.0000E+00
1.2800E-07	9.9627E-01
6.2400E-07	9.7994E-01
1.1840E-06	9.3093E-01
2.9600E-06	6.7610E-01
5.1200E-06	3.5920E-01
6.2400E-06	2.2688E-01
7.5200E-06	1.2234E-01
8.8000E-06	5.6996E-02
1.0048E-05	2.2692E-02
1.2000E-05	4.7230E-03
1.2800E-05	0.0000E+00
1.0182E-03	0.0000E+00



**Figure 3 Transmitter waveform for the Low Moment (LM) configuration (SkyTEM<sup>312</sup>)**

**Table 7 Detailed SkyTEM<sup>312</sup> HM transmitter current waveform**

Time [s]	Amplitude
-5.00000E-03	0.00000E+00
-4.79532E-03	6.52344E-01
-4.69386E-03	9.33594E-01
-3.82897E-03	9.49219E-01
-2.13784E-03	9.77344E-01
-7.26966E-04	9.94531E-01
-2.19939E-06	1.00000E+00
1.04316E-05	9.81961E-01
5.79841E-05	8.39282E-01
1.48063E-04	5.57539E-01
2.31183E-04	2.88357E-01
2.79509E-04	1.29935E-01
3.15850E-04	1.35143E-02
3.28993E-04	0.00000E+00


**Figure 4 Transmitter waveform for the High Moment (HM) configuration (SkyTEM<sup>312</sup>)**



### 2.3 Receiver Specifications

A summary of the receiver specifications are provided in Table 8. The locations of the X-component and Z-component receiver coils are provided in Table 3.

**Table 8 Summary of receiver specifications**

RECEIVER (Rx) SPECIFICATIONS	
Rx ID = TIB 025	SkyTEM <sup>312</sup>
EM Sensors	<i>dB/dt</i> coils
Rx coil effective area	175 m <sup>2</sup> (Z) 115 m <sup>2</sup> (X)
Low pass cut-off frequency for Rx coils	155 KHz (Z) 250 kHz (X)
Low pass cut-off frequency for Rx electronics	300 kHz
Front gate	0.00 µs (LM) 370.00 µs (HM)
Earliest gate centre time	16.09 µs (LM) Gates 9
Measured / recommended use	436.42 µs (HM) Gate 16
Latest gate centre time	0.877 ms (LM) Gate 26 13.16 ms (HM) Gate 38

### 2.4 EM Channel Times

Table 9 and Table 10 list the SkyTEM channel times. Both low moment (LM) and high moment (HM) were used for the survey. Times are measured from the start of current switch-off, i.e. from the top of the current ramp. Note that a calibration correction shift has been applied to the gate times. Refer to the Calibration Section in this document on page 13.

**Table 9 Detailed SkyTEM<sup>312</sup> LM channel times. All gate times are relative to the start of the transmitter current ramp down.**

LM Gate Number	Gate Width (μs)	Gate Open (μs)	Gate Centre (μs)	Gate Close (μs)
9	3.57	14.63	16.415	18.2
10	4.57	18.63	20.915	23.2
11	5.57	23.63	26.415	29.2
12	7.57	29.63	33.415	37.2
13	9.57	37.63	42.415	47.2
14	12.57	47.63	53.915	60.2
15	15.57	60.63	68.415	76.2
16	19.57	76.63	86.415	96.2
17	24.57	96.63	108.915	121.2
18	30.57	121.63	136.915	152.2
19	39.57	152.63	172.415	192.2
20	50.57	192.63	217.915	243.2
21	62.57	243.63	274.915	306.2
22	80.57	306.63	346.915	387.2
23	100.57	387.63	437.915	488.2
24	126.57	488.63	551.915	615.2
25	160.57	615.63	695.915	776.2
26	201.57	776.63	877.415	978.2

The following table lists the gate times for the receiver configurations used for the High Moment segment in the surveys.

**Table 10 SkyTEM<sup>312</sup> HM gate times. All gate times are relative to the start of the transmitter current ramp down.**

HM Gate Number	Gate Width (us)	Gate Open (us)	Gate Centre (us)	Gate Close (us)
16	19.57	426.63	436.415	446.20
17	24.57	446.63	458.915	471.20
18	30.57	471.63	486.915	502.20
19	39.57	502.63	522.415	542.20
20	50.57	542.63	567.915	593.20

HM Gate Number	Gate Width (us)	Gate Open (us)	Gate Centre (us)	Gate Close (us)
21	62.57	593.63	624.915	656.20
22	80.57	656.63	696.915	737.20
23	100.57	737.63	787.915	838.20
24	126.57	838.63	901.915	965.20
25	160.57	965.63	1045.915	1126.20
26	201.57	1126.63	1227.415	1328.20
27	254.57	1328.63	1455.915	1583.20
28	321.57	1583.63	1744.415	1905.20
29	405.57	1905.63	2108.415	2311.20
30	510.57	2311.63	2566.915	2822.20
31	645.57	2822.63	3145.415	3468.20
32	791.57	3468.63	3864.415	4260.20
33	967.57	4260.63	4744.415	5228.20
34	1184.57	5228.63	5820.915	6413.20
35	1451.57	6413.63	7139.415	7865.20
36	1775.57	7865.63	8753.415	9641.20
37	2179.57	9641.63	10731.42	11821.20
38	2669.57	11821.63	13156.42	14491.20

## 2.5 Interleaving of Transmitter Moments

All data were acquired using interleaved low and high moment transmitter modes, consisting of 110 low moment positive and negative pulse pairs at 275 Hz, and 30 high moment pulse pairs at 25Hz, which repeats every 1.6 seconds.

## 2.6 Sign Convention of the Data

### *EM data*

The vertical (Z) component electromagnetic data is referenced such that when measured over a purely-conductive (non-polarizable) one-dimensional earth it is positive. Early-time Z-component negatives are sometimes observed in very resistive areas due to the transmitter bias, if it has not been completely removed from the measured data. Late time Z-component negatives are occasionally observed due to induced polarization effects.

The horizontal inline (X) component electromagnetic data is positive in the flight direction: The X-component response measured over a purely-conductive (non-polarisable) one-dimensional earth is typically negative. However, X-component data is strongly affected by frame tilt, which can introduce a large contribution from the much-stronger Z-component response and significantly distort the measured X-component response. The only rigorous way to account for this effect in the data is to explicitly include the transmitter loop tilts in the X and Y directions in the forward/inverse modelling algorithm used to interpret the data.

### *Tiltmeter data*

Angle X (measured by both TL1 and TL2) is positive when the nose of the transmitter loop frame is pitched up, i.e. over level ground, Angle X is positive when the nose of the frame is further from the ground than the base of the tail rudder.

Angle Y (measured by both TL1 and TL2) is positive when the starboard (right) side of the transmitter loop frame is tilted down i.e. over level ground, Angle Y is positive when the starboard side of the frame is closer to the ground than the port side.

## 2.7 GPS Navigation System

Two Novatel OEMV GPS receivers were employed for the survey.

The OMNISTAR High Precision real time differential correction service was used to provide a real time input to GP2 for the primary navigation system.

As a backup, both GP1 and GP2 recorded information, for which differentially-corrected positions could be obtained via post-processing if required, in conjunction with data from a ground base station recorded at 1 second intervals.

## 2.8 Magnetometer System

### Airborne Magnetometer

Geometrics G822A

Caesium Vapour magnetometer sensor, mounted on the front of the Tx loop frame. (Figure 2)

Kroum VS KMAG4

Counter Sample interval 50 Hz. (Down sampled in processing)

### Base Magnetometer

GEM Systems GSM 19

Proton precession, sample interval 1 Hz

Typical noise level

0.5 nT

## 2.9 Magnetometer Base Station

The table below shows the locations of the magnetic base station.

**Table 11 The location for the base station magnetometer.**

Magnetometer	Lat	Lon
<b>Base station</b>		
Hayes Creek Serial No. 14	13° 31'21.91"S	131° 24'13.43"S

The base station magnetometer data were transferred into a base station Geosoft GDB database on a daily basis for further processing.

## 3. CALIBRATION

### 3.1 Reference Site Calibrations

The complete SkyTEM equipment was calibrated in May 2015 at the National Danish Reference Site (GeoFysikSamarbejdet, Aarhus University, 2012). The following plots, Figure 5 to Figure 10 show the measured data as well as the expected response at altitudes: 13 m, 15 m, 23 m, 26 m, 33 m, and 36 m.

Calibration factors and time shift are given below. These factors have been applied to the delivered EM data, and therefore the data do not need to be scaled or the window times do not need to be shifted prior to modelling/inversion.

LM:  
Factor 0.94  
Time shift -1.8 e-6 s

HM:  
Factor 0.94  
Time shift -1.8e-6  $\mu$ s

The reference data for both LM and HM data are shown as grey curves and the measured data for LM and HM as green and blue curves respectively.

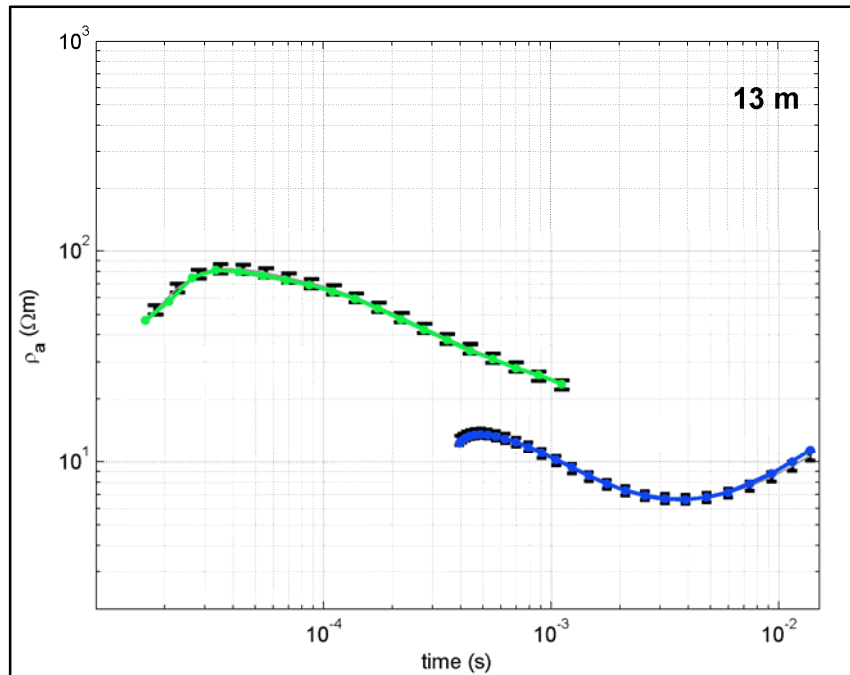


**Figure 5** The frame at 13 m altitude. Grey curves with 5% error bars are the expected response, and green curves (LM) and blue curves (HM) are the actual measurements.

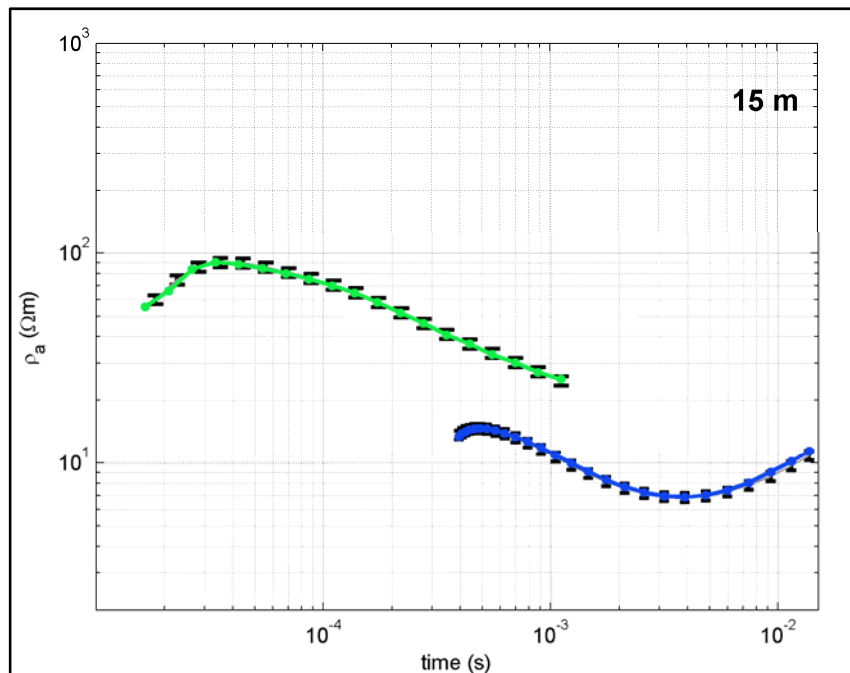


**Figure 6** The frame at 15 m altitude. Grey curves with 5% error bars are the expected response, and green curves (LM) and blue curves (HM) are the actual measurements.

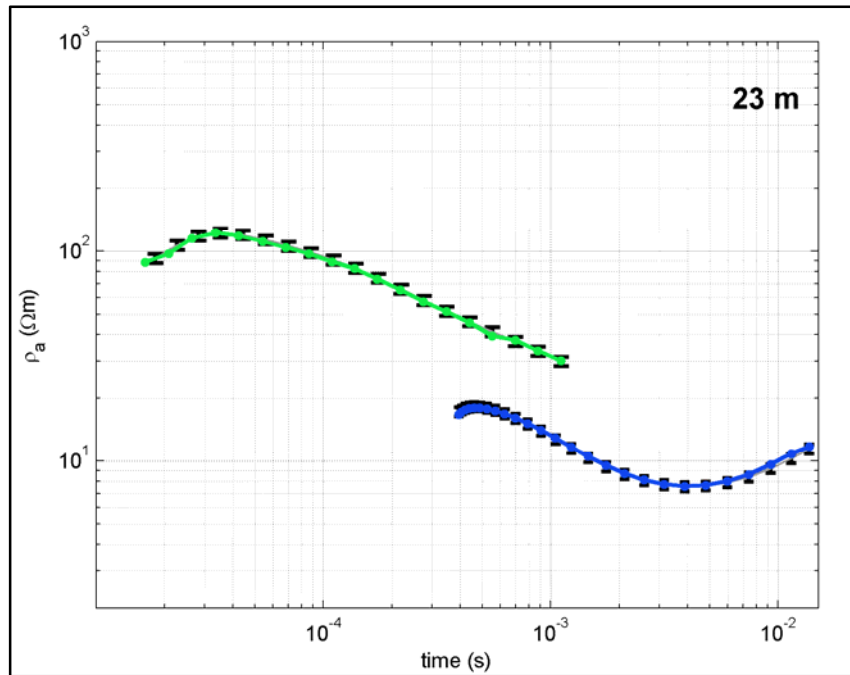


**Figure 7** The frame at 23 m altitude. Grey curves with 5% error bars are the expected response and green curves (LM) and blue curves (HM) are the actual measurements.

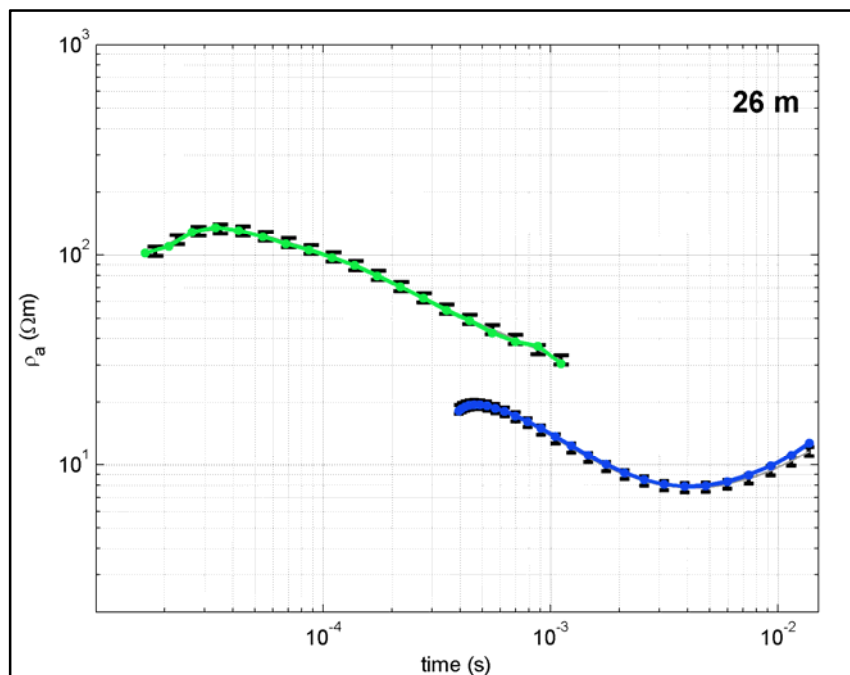


**Figure 8** The frame at 26 m altitude. Grey curves with 5% error bars are the expected response and green curves (LM) and blue curves (HM) are the actual measurements.

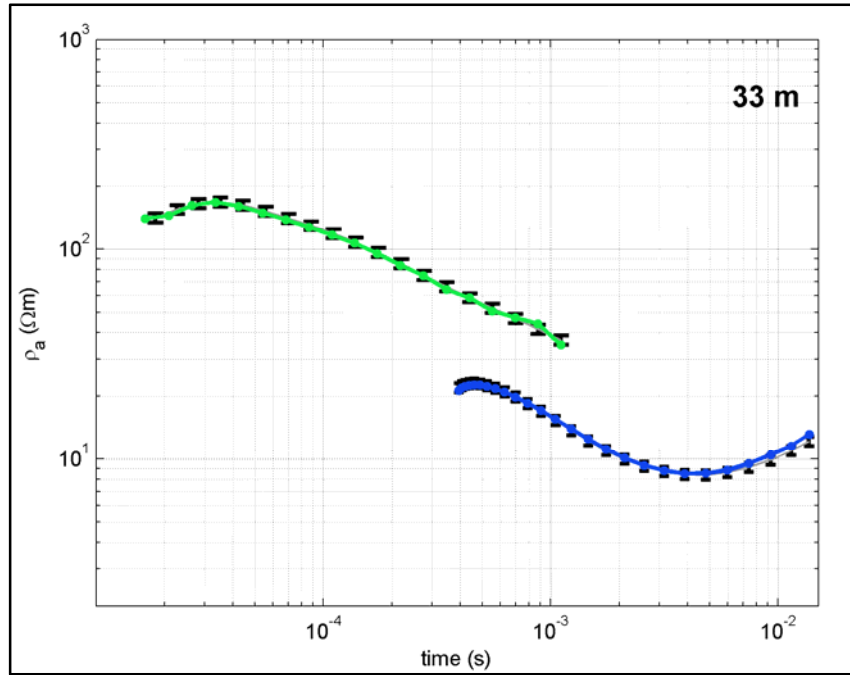


**Figure 9** The frame at 33 m altitude. Grey curves with 5% error bars are the expected response and green curves (LM) and blue curves (HM) are the actual measurements.

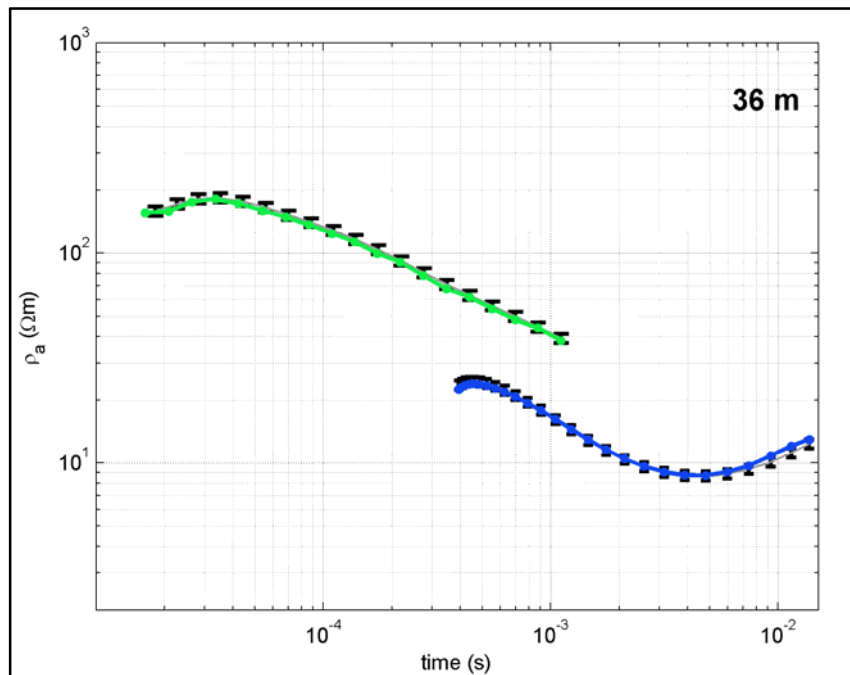


**Figure 10** The frame at 36 m altitude. Grey curves with 5% error bars are the expected response and green curves (LM) and blue curves (HM) are the actual measurements.



### 3.2 Laser Altimeter Calibration

**Table 12 Results of the laser altimeter calibration**

#### Laser Altimeter Calibration Test

Performed by: Wade Markow 14/6/2017

Equipment Used -

Tajima Symron-R 100m Fiberglass Measuring Tape 20N. Serial Number - JQCN08001

Stanley TLM 165 TRU-LASER MEASUREMENT 50m. Accuracy  $\pm 1.5\text{mm}$

Laser Altimeter #5026 - LaserAce IM HR

Laser Altimeter #6035 - LaserAce IM HR

100m Fibreglass Measuring Tape	Laser #5026	Laser #6035	Stanley 50m Handheld Laser
(metres)	(metres)	(metres)	(metres)
10	10.0	10.0	10.0
20	20.2	20.0	20.0
30	30.0	29.9	30.1
40	40.1	40.1	40.1
50	50.1	50.1	50.0
60	60.2	60.1	
80	79.9	79.9	
100	99.8	100.1	
120	119.9	120.1	

The calibration of the redundant laser altimeter systems, used to provide pilot guidance, and the calculation of the final digital elevation model were performed on the 14<sup>th</sup> June 2017.



**Figure 11 Calibration plot for laser #5026**

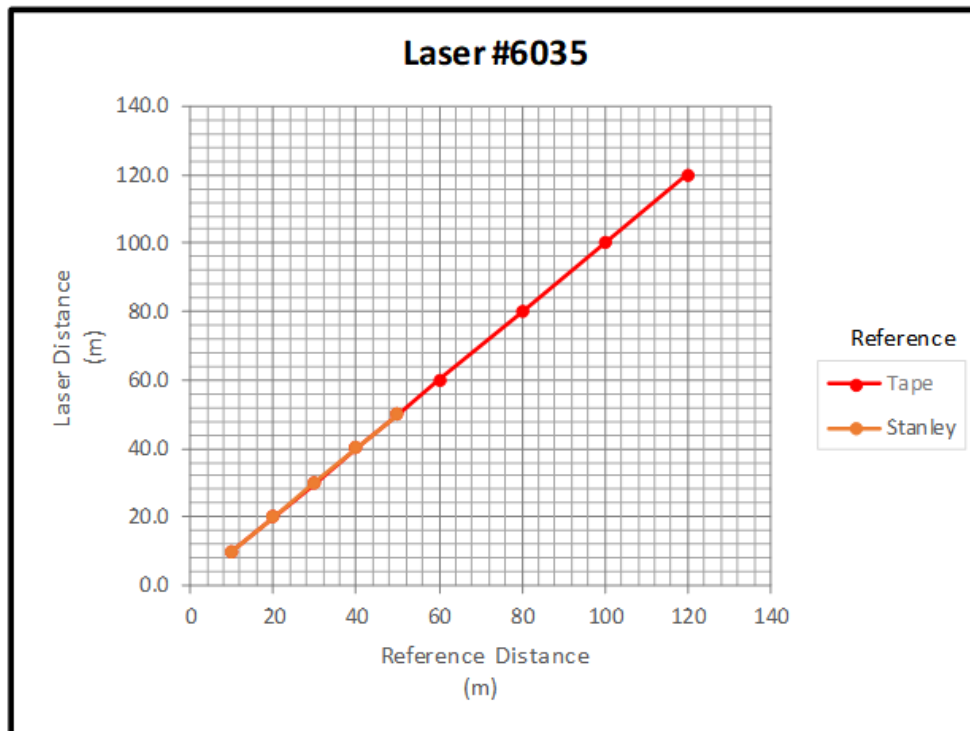


**Figure 12 Calibration plot for laser #6035**

### 3.3 Frame Inclinator Calibration

**Table 13 Inclinator calibration results**

#### Inclinator Calibration

Performed by: Wade Markow 14/6/2017

Equipment Used -

Bosch Level DNM 60L Professional - Accuracy  $-0^{\circ}/90 \pm 0.05^{\circ}$ ,  $-1-89^{\circ} \pm 0.2^{\circ}$

Inclinator: #7422

Inclinator: #7439

Inclinator #7439		Inclinator #7422		Bosch Level
X	Y	X	Y	°
°	°	°	°	
0.0	N/A	0.0	N/A	0.0
1.1	N/A	1.0	N/A	1.1
2.1	N/A	2.0	N/A	2.0
2.9	N/A	3.2	N/A	2.9
4.1	N/A	4.0	N/A	4.0
4.9	N/A	5.0	N/A	5.2
10.0	N/A	10.1	N/A	10.1
15.1	N/A	15.1	N/A	15.0
30.1	N/A	30.0	N/A	30.3
N/A	0.1	N/A	0.0	0.2
N/A	1.1	N/A	1.0	0.9
N/A	4.9	N/A	5.1	5.3
N/A	10.0	N/A	9.9	9.8
N/A	15.0	N/A	15.0	15.1
N/A	30.0	N/A	30.1	29.9

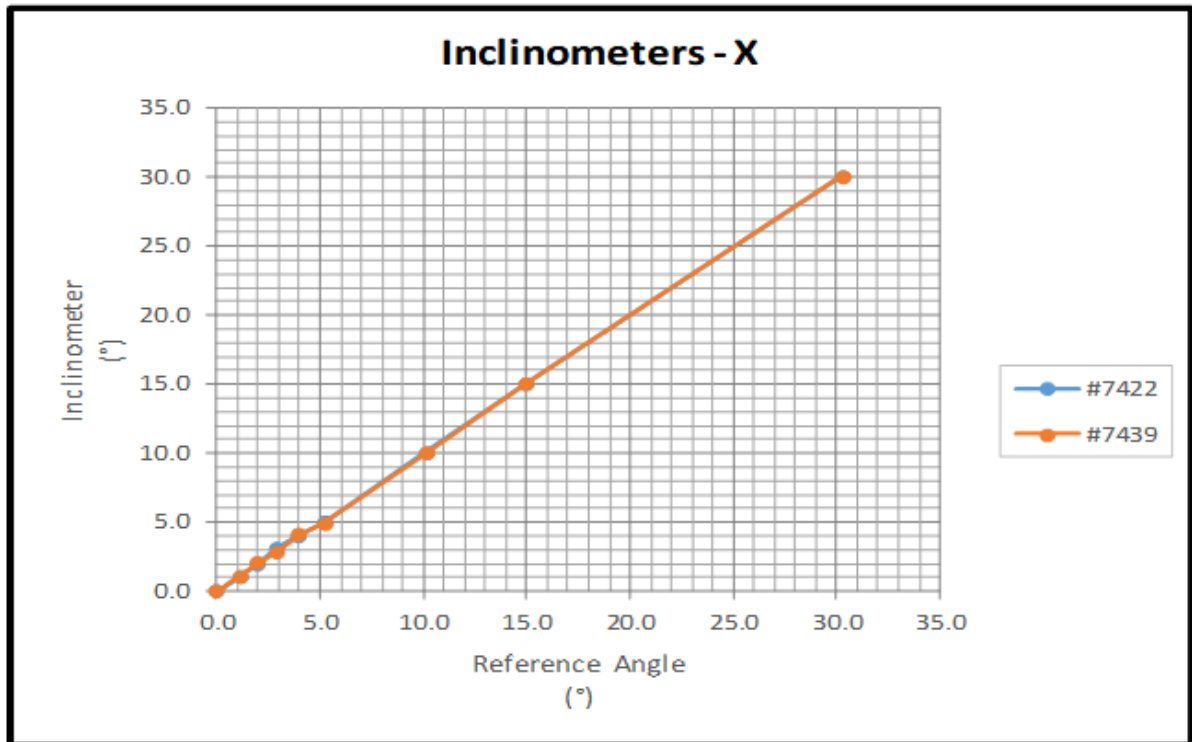


**Figure 13 Plot of X angle inclinometers against the Bosch reference**

Note that the lines overlies each other in the graphs.

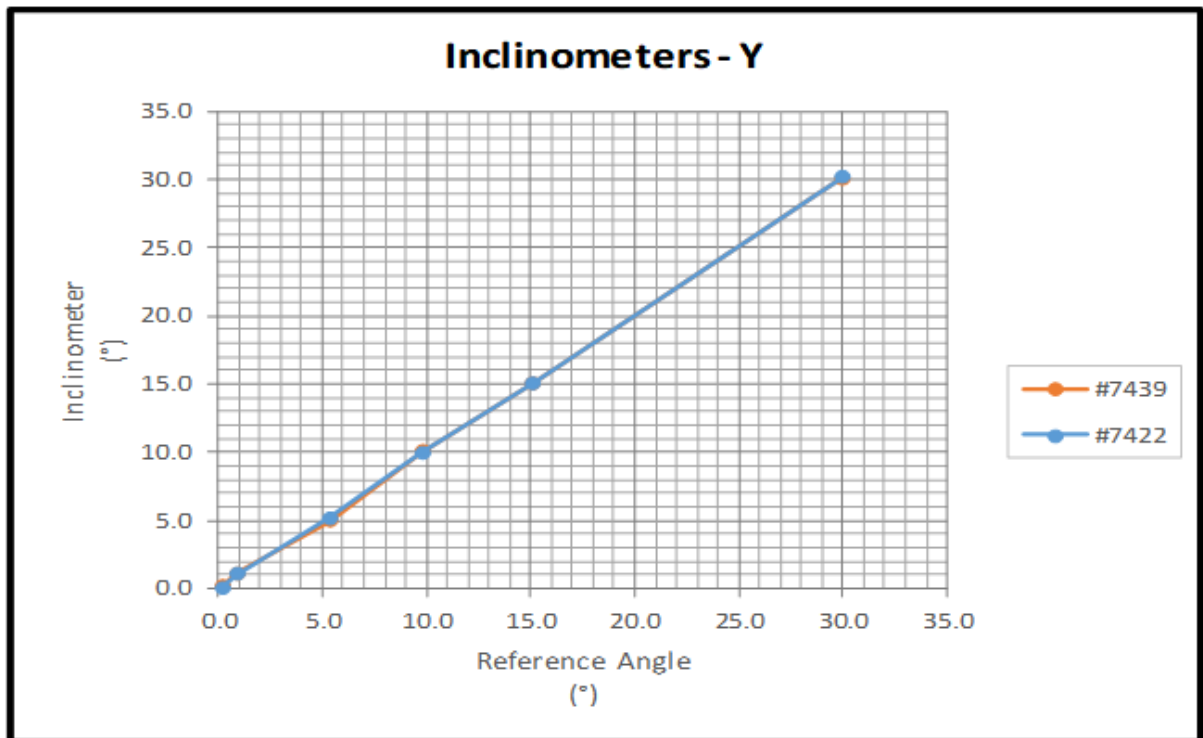


**Figure 14 Plot of Y angle inclinometers against the Bosch reference**

#### 4. POWER LINE NOISE INTENSITY

The PLNI monitor values are derived from a frequency analysis of the raw Z-component EM data. For every low moment EM data block (110 pulse pairs) a PLNI value is obtained by Fourier transformation of the measured values of the latest low moment gate. The Fourier transformation is evaluated at the local power transmission frequency (50 Hz) yielding the amplitude spectral density of the power line noise.

CAUTION - When evaluating the PLNI values one should be aware of the following factors that may give rise to anomalous PLNI patterns unrelated to the actual power line noise level:

- Noise sources, other than power line noise, may contribute to the total noise spectral density in the data at the power transmission frequency. When power line noise is present it tends to dominate all such other noise sources.
- The PLNI values are not corrected for flying height or frame angles, which means that adjacent lines crossing the same power line may not exhibit the same values of PLNI.

## 5. DATA PROCESSING

### 5.1 GPS Positions and Coordinates

Only the Omnistar HP differentially corrected GPS, GP2 position information were used for the survey. The data were recorded in the WGS84 datum.

The GPS positions were then translated to the centre of the frame based on the instrument x, y and z positions given in Table 3.

The corrected positions were transformed to GDA94 datum, Map Grid of Australia Zone 52 Projection

### 5.2 Laser Altimeter Data

The height processing involves manual and automated routines using a combination of the SkyTEM in-house software SkyLab and Oasis Montaj Geosoft.

The processing involves the following steps:

Keeping the 5 largest of the 30 values acquired per second, and discarding the remainder to correct for the canopy effect (treetop filter);

3 sec running box-car filter (smoothing filter);

Tilt correction, using the inclinometer data, to account for the altimeter not pointing vertically downward;

Averaging of the tilt corrected values from the two laser altimeters;

A 3 sec low pass filter is then applied to the final result.

### 5.3 Digital Elevation Model

The digital terrain model (DTM\_AHD) was derived by subtracting the processed laser altimeter (height above ground) data from the GPS altitude (height above the GRS80 ellipsoid) data to yield the height of the ground above the GRS80 ellipsoid. Then the ellipsoid-geoid separation (N-value) was subtracted to yield the elevation of the ground above the Australian Height Datum (AHD).

$$\text{Elevation}_{\text{AHD}} = \text{GPS\_Height}_{\text{GRS80}} - \text{Laser\_Altimeter} - \text{N\_Value}$$

The subtracted N-values were interpolated from the AUSGeoid09 grid values obtained via the Geoscience Australia website:

<ftp://ftp.ga.gov.au/geodesy-outgoing/gravity/ausgeoid/>

### 5.4 Electromagnetic Data

Raw (binary) SkyTEM data have been processed using SkyTEM proprietary software.

Prior to processing, primary field correction (PFC) was applied to the early LM moment gates (9 to 14) to remove the effects of residual currents that occur due to magnetic coupling between the receiver coils and the transmitter loop. PFC is performed by collecting Low Moment data whilst flying the system so the LM response is clear of any influence from the ground. The primary magnetic field coupling between the receiver coils and the transmitter loop is continuously hardware-monitored, providing a separate value for the magnetic field coupling during each transient sounding. These data are used for raw data correction in a separate post-processing step. The primary field compensation technique has

proven stable and has routinely yielded a reduction of the primary field influence in very early time gates by a factor exceeding 17dB.

Following PFC on the Low Moment data the data are normalized in respect to the effective Rx coil area, Tx coil area, number of turns and current giving the units  $[pV/(m^4 \cdot A)]$ .

The EM data is filtered adaptively, based on the signal-to-noise ratio. The applied EM filtering method is based on iterative weighted spline fitting routines, which operate in positive/negative symmetric transform spaces. The data weighting scheme relies on an extensive noise evaluation performed on the individual gate values of the raw data decays. Optimised sets of averaging filters are used for each measured moment and type of receiver coil in a stepwise averaging process. This allows for optimal suppression of motion induced noise as well as cultural noise components, while keeping track of the resulting data uncertainty.

## 5.5 Magnetic Data

Final processing of the magnetic data involved the application of conventional corrections to compensate for diurnal variation, International Geomagnetic Reference Field (IGRF) removal, and heading effects prior to gridding. Processing of magnetic data was implemented in Geosoft's Oasis Montaj software. The steps involved follow, with the details provided thereafter:

- Pre-processing of static (1 Hz) magnetic data acquired at the magnetic base stations
- Pre-processing of airborne magnetic data
- Standard corrections to compensate the diurnal variation.
- IGRF correction
- Gridding
- Grid levelling.

### *Pre-processing*

Pre-processing of the airborne magnetic data involved resampling of data to 2 Hz and translation of the position to the center of the transmitter frame in SkyLab. The data were then manually edited to remove spikes and other spurious data. The data were then low-pass filtered using a filter of 3.0 s width.

### *Diurnal correction*

Correction for the diurnal variation was made using the digitally recorded ground base station magnetometer data. The ground base station data were first manually de-spiked then low-pass filtered with a filter width of 10 s. The pre-processed base station data, which represent short term temporal magnetic field variations, were merged together with the airborne magnetic data using the date and UTC time as the synchronization channels.

These base station data were then subtracted from the airborne magnetometer readings. Then a constant value of 46469 nT was added back into the result. The resultant delivered data field from this step is the Total Magnetic Intensity (TMI).

### *IGRF correction*

The Geosoft Oasis Montaj Levelling Toolkit was used for applying the IGRF corrections to the magnetic data. The IGRF is a long-wavelength regional magnetic field calculated from permanent observatory data collected around the world. The IGRF is updated and determined by an international committee of geophysicists every 5 years. Secular variations in the Earth's magnetic field are incorporated into the determination of the IGRF. The IGRF correction was applied prior to levelling. The applied corrections were calculated using the following IGRF model parameters:

- IGRF model year: IGRF 12<sup>th</sup> generation
- Date: variable according to date channel in database

Date: 13 January 2018	Doc. No: AUS_10027	Page 23 of 31
-----------------------	-----------------------	---------------

- Position: variable according to GPS longitude and latitude
- Elevation: variable according to magnetic sensor altitude derived from DGPS data.

The resultant delivered data field from this step is the IGRF corrected TMI (TMI\_IGRF).



## 6. INVERSION OF THE SkyTEM DATA

Following is a description of modelling and inversion of SkyTEM data acquired during the survey.

### 6.1 Outline

The SkyTEM data have been inverted with the AarhusInv program (Auken et al., 2015) using the Aarhus Workbench LCI algorithm (Auken et al. 2005; Auken et al. 2002), a group of time-domain EM (TEM) soundings are inverted simultaneously using 1-D models (Kirkegaard and Auken, 2015). Each sounding yields a separate layered model, but the models are constrained laterally.

The result of the LCI inversion is a quasi-2D model section that varies smoothly along the profile and yields a conductivity model that combines the very good shallow depth resolution offered by the low moment data and the larger depth of investigation from the high moment data.

### 6.2 Input data and noise

The input data to the inversion were LM gates 9 to 26 and all HM gates of the Z-component. The manual masking of portions of data thought to contain coupling effects (e.g. due to power lines) was not a requirement of the project. Accordingly cultural effects in the EM data could be manifested in the inversion results and final conductivity database. Also negative decays can be observed in both LM and HM Z component response which could possibly due to IP effect. At present Aarhus Workbench does not resolve non-linear resistive properties.

A nominal uncertainty of 3% was applied to each datum, as well as the calculated relative uncertainty as provided with the EM data.

### 6.3 Model parameterization and initial model

The LCI code was run in multi-layer, smooth-model mode. In this mode the layer thicknesses are kept fixed and the data are inverted only for the resistivity of each layer. Inversion for flight altitude is also included after the first 5 inversion iterations. Multi-layer smooth-model inversion is slower to compute, but is usually able to provide a very close fit to the observed data.

For this survey a 30 layer model was used, in which the bottommost layer is an infinitely thick halfspace. The thickness of the topmost layer was set to 5 m and the depth to the top of the bottommost (halfspace) layer was set to 600 m. The layer thicknesses increase logarithmically with depth. The thicknesses and depths to the top of each layer are given in Table 14.

The initial model resistivity structure was a homogenous half-space model with an auto calculated starting resistivity. This resistivity is the mean of the apparent resistivities calculated for each sounding.

**Table 14 Conductivity model layer thicknesses**

Layer #	Layer Thickness [m]	Depth to top of layer [m]	Res. Constraints Vert.	Res. Constraints Horz.
1	5.0	0.0	2.00	1.600
2	5.4	5.0	2.00	1.600
3	5.8	10.4	2.00	1.600
4	6.3	16.2	2.00	1.600
5	6.7	22.5	2.00	1.600
6	7.3	29.2	2.00	1.500
7	7.8	36.5	2.00	1.500
8	8.4	44.3	2.00	1.500
9	9.1	52.8	2.00	1.500
10	9.8	61.9	2.00	1.400
11	10.6	71.7	2.00	1.400
12	11.4	82.3	2.00	1.400
13	12.3	93.7	2.00	1.400
14	13.2	105.9	2.00	1.400
15	14.3	119.2	2.00	1.400
16	15.4	133.5	2.00	1.400
17	16.6	148.8	2.00	1.300
18	17.9	165.4	2.00	1.300
19	19.3	183.3	2.00	1.300
20	20.8	202.6	2.00	1.300
21	22.4	223.3	2.00	1.300
22	24.1	245.7	2.00	1.300
23	26.0	269.8	2.00	1.300
24	28.0	295.8	2.00	1.300
25	30.2	323.8	2.00	1.300
26	32.5	354.0	2.00	1.300
27	35.1	386.6	2.00	1.300
28	37.8	421.6	2.00	1.300
29	40.7	459.4	2.00	1.300
30	∞	500.2	2.00	1.300

#### 6.4 Regularization

Smoothness constraints are applied on the variation of resistivity with depth. In addition lateral constraints are applied between adjacent models.

Constraints are given as factors, i.e. a factor of 1.1 means that the parameter can vary between the starting value divided by 1.1 to the starting value multiplied by 1.1 (Aarhus University, n.d.).

The LCI inversion allows for horizontal and vertical constraints to be set for resistivities. For this survey, the vertical resistivity constraints were set to 2.0. So for each iteration, the resistivity of the layer above, and below each layer can be between [2 X initialRes], or [0.5 X initialRes].

Horizontal constraints are scaled by distance using a reference distance and power function:

$$C = 1 + \left( C_{opt} - 1 \right) \left( \frac{\Delta GPS}{Dist_{ref}} \right)^n$$

Where  $C$  is the constraint used scaled by distance,  $C_{opt}$  is the optimal constraint at a sounding distance of  $Dist_{ref}$  and  $\Delta GPS$  is the actual sounding distance. For this survey,  $C_{opt}$  is the horizontal constraint given in Table 14, and  $Dist_{ref} = 25$  m. The power law dependency  $n$ , was set to one. Note that these constraints are not strict, and do not prevent abrupt changes, if fitting of the data requires it.

The constraint on the inverted flight height was set to 1.3.

## 6.5 Depth of investigation

The depth of investigation (DOI) is determined by performing a sensitivity analysis of the cumulated response of the data to each layer's resistivity from the deepest layer upwards, (Christiansen and Auken, 2012).

## 6.6 Qualifications on the conductivity model

Geophysical inversion is a non-unique process. This means that many possible conductivity models could possibly explain the data. Several factors contribute to this non-uniqueness, some of which are outlined below.

### *Data and noise model*

The accuracy of conductivity model generated by the inversion is influenced by the noise in the TEM data. This noise is reduced by selective stacking of delay time series and by applying appropriate filters in the receiver system, nevertheless noise is present in the data.

### *Data insufficiency*

For SkyTEM data, the insufficiency lies primarily in the limited delay time range that can be obtained. The earliest obtainable time gate is determined by the turnoff of the Tx current, and the latest useful time gate is determined by the signal to noise ratio. Increasing the Tx moment will give better measurements at late times, and thus improve the depth penetration, but also increase the turnoff time and thus remove early-time gates, thereby making the near-surface resolution poorer. This trade-off is partially solved by transmitting an alternating sequence of (1) a low moment that can be turned off quickly to give good near-surface resolution, and (2) a high moment that will improve the signal-to-noise ratio at late times, thus improving depth penetration.

### *Inconsistency between 1D modelling and 3D geology*

When using 1D modelling in the inversion of SkyTEM data, inconsistency arises where the lateral gradient of conductivity is large, e.g. typically in mining applications. However, also in environmental investigations, inconsistencies can arise, typically where strong near-surface conductors have abrupt boundaries.

Often such inconsistency is indicated by the data residual being high. One should look upon the inversion results with some caution at these locations. 3D effects can also reveal themselves by the so-called 'pant legs', i.e. conductive or resistive structures projecting at an angle of approximately 30 degrees from the horizontal at the edges of high contrast structures.

## 6.7 Conductivity Model Sections

The models resulting from the inversion are presented as sections of conductivity - depth intervals and are delivered in digital format.

### *Model sections*

The model sections can be found in the data delivery folder as PNG and PDF format

The main section plots consist of four subplots as seen in Figure 15. The top plot displays the inverted models, with topography, where the conductivity of the individual layers are colour coded according to the colour scale bar, which is displayed using a logarithmic distribution. The black line on the section indicates the estimated depth of investigation (DOI).

The measured and inverted flight elevation are shown with a black and blue line, respectively, above the model section.

In each section, the region below the estimate of the DOI, the inverted conductivity is determined predominantly by the regularization, i.e. the conductivity is essentially undetermined.

Underneath the model section plot are two plots of the measured data (dots) together with the response of the inverted models (solid lines). LM is low moment data and HM is high moment data. The bottom plot is the data residual (black line) of the inversions.

Blank sections in the data profile indicate areas where the signal to noise ratio has been too low for any data to be used in the inversion. Essentially the resistivity in those sections can be considered as “Very high” ( $>1000 \Omega\text{m}$ ). Alternatively cultural features have been superimposed on the ground response, which can also lead to data being discarded prior to the inversion.

### Residuals

The quality of the fit between the observed data and the predicted data (i.e., the calculated forward model response of the conductivity model resulting from the inversion) can be evaluated by inspecting the residuals. The data residual is calculated by comparing the measured data with the response of the resulting model after inversion. If the residual is in the vicinity of 1, the misfit between the response of the final model and the data is, on average, equal to the noise. A high residual is due to data that has noise greater than the noise model takes into account. This can be seen where resistivities are very high and the signal consequently very low. A high data residual can also be due to the inconsistency between the 1D model assumed in the inversion and the 2D/3D character of the real world geology. These are found primarily at the edges of sharp lateral conductivity contrasts. Finally, coupling effects due to power lines and other man made conductors can also be a source of a high residual.

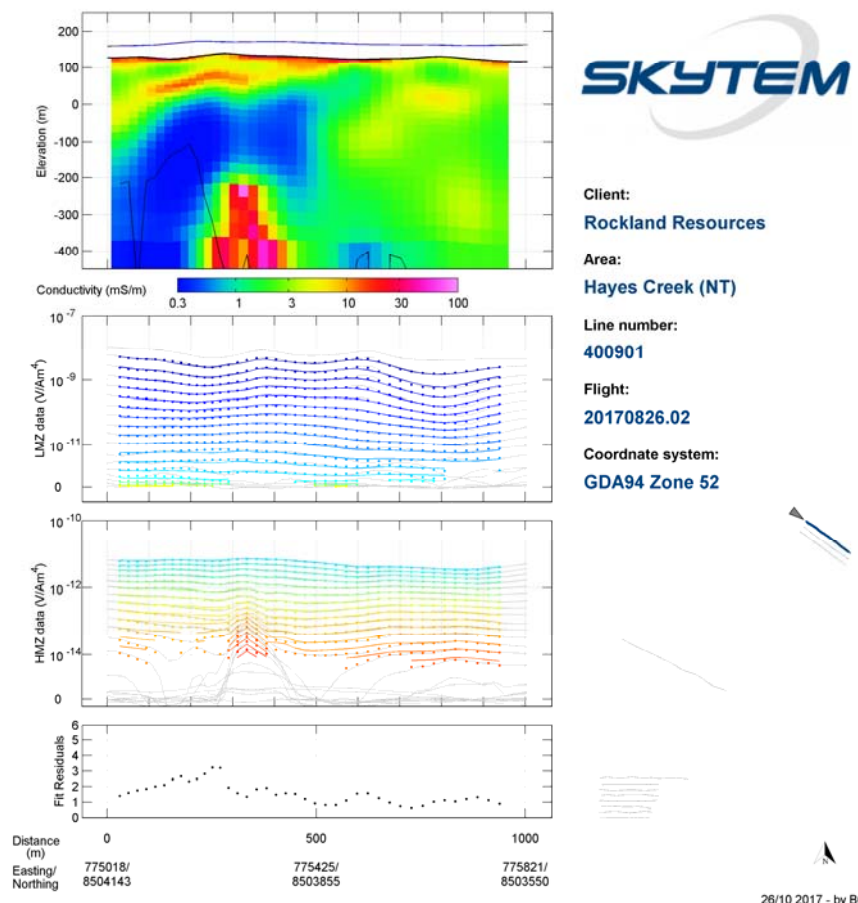


**Figure 15 Model section. From top to bottom: Conductivity section with flight height and Depth of Investigation (DOI), LM gate plot (data=dots, model=line), HM gate plot (data=dots, model=line), data residual.**

## 7. DELIVERED REPORT AND DATA

### 7.1 Report

#### Acquisition and Processing Report

**Format** PDF

**Copies** 1 × Electronic copy

### 7.2 Electromagnetic data

**AUS\_10027\_HayesCk\_EM Geosoft .gdb & ASCII .xyz**

FIELD	CHANNEL	DESCRIPTION	UNITS
1	Fiducial	Fiducial Number	s
2	Line	Line number	
3	Flight	Flight number	
4	DateTime	Decimal Days since midnight 31/12/1899	days
5	Date.UTC	UTC Date	yyyymmdd
6	Time.UTC	UTC Time	hhmmss.ss
7	AngleX	Tilt of frame from horizontal - flight direction	deg
8	AngleY	Tilt of frame from horizontal - perpendicular from flight direction	deg
9	Height	Laser altimeter measured height of the Tx loop centre above ground	m
10	DTM_AHD	Digital terrain model (Australian Height Datum)	m
11	Longitude	Longitude GDA94	deg
12	Latitude	Latitude GDA94	deg
13	Easting	Easting (GDA94 MGA Zone 52)	m
14	Northing	Northing (GDA94 MGA Zone 52)	m
15	GPS_Alt	GPS altitude of Tx loop centre (GRS80 datum)	m
16	GdSpeed	Frame ground speed	km/h
17	Curr_LM	Low moment peak transmitter current	A
18	Curr_HM	High moment peak transmitter current	A
19	PLNI	Power line noise indicator	
20:45	LM_Z	Z-comp LM dB/dt processed and normalised (Gates 1-8 undefined)	pV/A.turns.m4
46:83	HM_Z	Z-comp HM dB/dt processed and normalised (Gates 1-15 undefined)	pV/A.turns.m4
84:109	LM_X	X-comp LM dB/dt processed and normalised (Gates 1-8 undefined)	pV/A.turns.m4

FIELD	CHANNEL	DESCRIPTION	UNITS
110:147	HM_X	X-comp HM dB/dt processed and normalised (Gates 1-15 undefined)	pV/A.turns.m4
148:173	RUNC_LM_Z	Z-comp LM dB/dt relative uncertainty (noise estimate as a fraction of the measured response)	
174:211	RUNC_HM_Z	Z-comp HM dB/dt relative uncertainty (noise estimate as a fraction of the measured response)	
212:237	RUNC_LM_X	X-comp LM dB/dt relative uncertainty (noise estimate as a fraction of the measured response)	
238:275	RUNC_HM_X	X-comp HM dB/dt relative uncertainty (noise estimate as a fraction of the measured response)	
276	MA1	Raw magnetic field reading	nT
277	BMAG	Base station diurnal magnetic field	nT
278	TMI	Total Magnetic field intensity + 46469.47 nT constant	nT
279	IGRF	International Geomagnetic Reference Field	nT
280	TMI_IGRF	TMI corrected by IGRF + 46469.47 nT constant	nT

### 7.3 Conductivity data

HayesCk\_WB\_MGA52

Geosoft (.gdb) & ASCII (xyz) NULL=-1e32

FIELD	CHANNEL	DESCRIPTION	UNITS
1	Fiducial	Fiducial Number	s
2	DateTime	Decimal Days since midnight 31/12/1899	days
3	Line	Line number	
4	Easting	Easting (GDA94 MGA Zone 52)	m
5	Northing	Northing (GDA94 MGA Zone 52)	m
6	DTM_AHD	Digital terrain model (Australian Height Datum)	m
7	RESI1	Residual of the data	
8	HEIGHT	Laser altimeter measured height of the Tx loop centre above ground	m
9	INVHEIGHT	Calculated inversion height of the Tx loop centre above ground	m
10	DOI	Estimated Depth of investigation, below ground level	m
11:40	Elev	Elevation to the top of the layer	m
41:70	Con	Conductivity of the layer	mS/m
71:100	Con_doi	Conductivity of the layer masked to the depth of investigation	mS/m
101:130	RUnc	Calculated relative uncertainty of the layer conductivity	

LCI conductivity sections		
Format	Image (.png) and PDF	
	Name	Description
	LineZZZZZZ_Cond_0.0003_0.1S_pr_m	Conductivity-depth sections ZZZZZZ = Line number

## 8. REFERENCES

Aarhus University, n.d., Guide to 1D-LCI inversion.

Auken, E., Foged, N. and Sørensen, K., 2002, Model recognition by 1-D laterally constrained inversion of resistivity data: Proceedings – New Technologies and Research Trends Session, 8<sup>th</sup> meeting, EEGS-ES.

Auken, E., Christiansen, A. V., Jacobsen, B. H., Foged, N., and Sørensen, K. I., 2005, Piecewise 1D Laterally Constrained Inversion of resistivity data: *Geophysical Prospecting*, 53, 497–506.

Auken, E., Christiansen, A. V., Kirkegaard, C., Fiandaca, G., Schamper, C., Behroozmand, A. A., Binley, A., Nielsen, E., Effersø, F., Christensen, N. B., Sørensen, K., Foged, N., Vignoli, G., 2015, An overview of a highly versatile forward and stable inverse algorithm for airborne, ground-based and borehole electromagnetic and electric data: *Exploration Geophysics*, 46, 223 – 235.

Christiansen, A.V. and Auken, E., 2012, A global measure for depth of investigation: *Geophysics*, vol 77, No. 4, 171-177.

GeoFysikSamarbejdet Aarhus University, 2012, Refinement of the National TEM reference model at Lyngby June 2012 (update from Nov. 2011)

Kirkegaard, C., and Auken, E., 2015, A parallel, scaleable and memory efficient inversion code for very large-scale airborne electromagnetic surveys: *Geophysical Prospecting*, 63, 495-507.